ACS central science

Research Article

http://pubs.acs.org/journal/acscii

General Synthetic Method for Si-Fluoresceins and Si-Rhodamines

Jonathan B. Grimm, Timothy A. Brown, Ariana N. Tkachuk, and Luke D. Lavis*

Janelia Research Campus, Howard Hughes Medical Institute, Ashburn, Virginia 20147, United States

Supporting Information

ABSTRACT: The century-old fluoresceins and rhodamines persist as flexible scaffolds for fluorescent and fluorogenic compounds. Extensive exploration of these xanthene dyes has yielded general structure−activity relationships where the development of new probes is limited only by imagination and organic chemistry. In particular, replacement of the xanthene oxygen with silicon has resulted in new red-shifted Si-fluoresceins and Si-rhodamines, whose high brightness and photostability enable advanced imaging experiments. Nevertheless, efforts to tune the chemical and spectral properties of these dyes have been hindered by difficult synthetic routes. Here, we report a general strategy for the efficient preparation of Si-fluoresceins and Si-rhodamines from readily synthesized bis(2-bromophenyl)silane intermediates. These dibromides undergo metal/bromide exchange to give bis-aryllithium or bis(aryl Grignard) intermediates, which can then add to anhydride or ester electrophiles to afford a variety of Si-xanthenes. This strategy enabled efficient (3−5 step) syntheses of known and novel Si-fluoresceins, Si-rhodamines, and related dye structures. In particular, we discovered that previously inaccessible tetrafluorination of the bottom aryl ring of the Si-rhodamines resulted in dyes with improved visible absorbance in solution, and a convenient derivatization through fluoride-thiol substitution. This modular, divergent synthetic method will expand the palette of accessible xanthenoid dyes across the visible spectrum, thereby pushing further the frontiers of biological imaging.

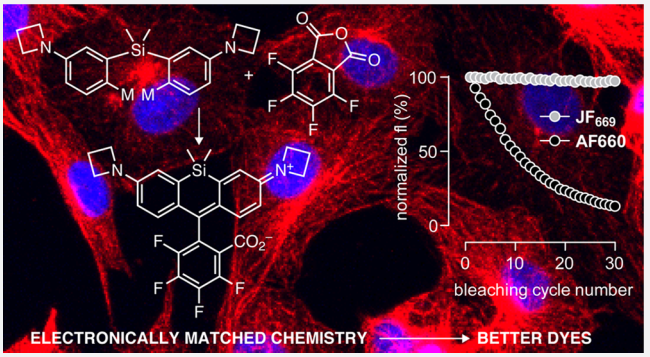

Chemical fluorophores are vital tools for biological research. The ability to modulate fluorophore properties using chemistry allows the fine-tuning of dyes for specific applications. In particular (and despite their age[1,2]), the fluorescein and rhodamine dyes enjoy a privileged status as versatile scaffolds for a variety of biological probes:[3−6] cellular stains,[7,8] biomolecular labels,[9−17] reversible[18−21] and irreversible[22,23] indicators, fluorogenic enzyme substrates,[24−28] and photoactivatable dyes.[29−35] This broad utility of the xanthene fluorophores stems from two properties: (i) the "open−closed" equilibrium between a highly absorbing, fluorescent, zwitterionic (Z) form and a colorless, nonfluorescent, lactone (L) form (Figure 1a), which allows construction of fluorogenic[36] molecules; (ii) the ability to modulate the spectral properties by either extending conjugation[11,13] or replacing the xanthene oxygen with a carbon,[37−41] silicon,[15−17,42−55] phosphorus,[56,57] or sulfur.[58] Over a century of chemistry has provided a general framework for structure−activity relationships for these scaffolds, where specific modifications to fluoresceins and rhodamines can elicit predictable changes in the spectral and chemical properties of the resulting dyes.

The silicon substituted xanthene dyes have emerged as exceptionally useful probes for biological imaging. Replacement of the central xanthene oxygen atom with an SiR_2 moiety results in ∼100 nm bathochromic shifts in the absorption maximum (λ_{max}) and fluorescence emission maximum (λ_{em}), providing "Si-fluorescein" (SiFl, **1**, Figure 1a) and "Si-rhodamine" (SiRh) analogues;[15−17,42−55] the hybrid "Si-rhodol" system is also useful.[59−61] Interestingly, introduction of the Si moiety also alters the open−closed equilibrium of both scaffolds, with SiFl and SiRh dyes preferentially adopting the lactone form relative to the parent fluorophores.[15,46,49] The unique properties of Si-xanthene dyes have been exploited to prepare sophisticated fluorescent probes used at the forefront of modern microscopy methods, including novel fluorogenic labels[16,46] and stains[8,47,50] for cellular imaging, far-red voltage indicators,[52] and sensors for disparate analytes.[45,60,61] In previous work, we discovered that replacement of standard *N*,*N*-dialkylamino moieties with four-membered azetidine rings was a general strategy to improve fluorophore brightness without significantly altering λ_{max} or λ_{em}.[15] We applied this strategy to the SiRh system, resulting in the development of "Janelia Fluor 646" (JF_{646}, **3**, Figure 1a). The superior brightness, photostability, and fluorogenicity of this dye have made it a useful tool for single-particle tracking experiments in vitro[62] and in live cells.[63,64] Subsequent development of a photoactivatable derivative ("PA-JF_{646}") has greatly extended its capabilities for super-resolution localization microscopy.[35]

A significant problem in the development of new SiFl and SiRh derivatives is chemistry—the extant synthetic strategies are inefficient and laborious. For example, our original synthesis

Received: June 12, 2017
Published: August 9, 2017

DOI: 10.1021/acscentsci.7b00247
ACS Cent. Sci. 2017, 3, 975−985

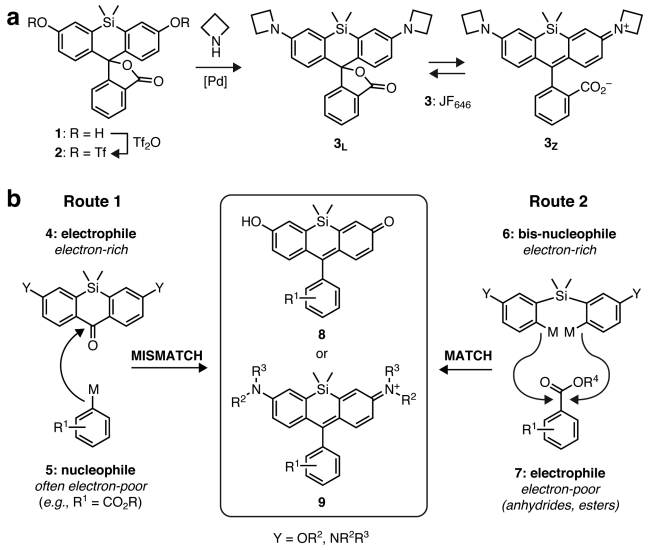

Figure 1. Synthetic strategies for Si-fluoresceins and Si-rhodamines. (a) Cross-coupling synthesis and lactone−zwitterion equilibrium of JF_{646} (**3**). (b) Two general approaches for the preparation of Si-fluoresceins and Si-rhodamines.

of JF_{646} (**3**) used a straightforward Pd-catalyzed cross-coupling of azetidine with the ditriflate (**2**) of SiFl (**1**, Figure 1a). The preparation of **1**, however, is relatively long and low-yielding (6.0% yield, 9 steps), resulting in a poor overall yield for JF_{646} (4.6% yield, 11 steps, Figure S1a).[15] This has hindered our efforts to further optimize and modulate the properties of SiFl or JF_{646} dyes for fluorescence imaging experiments. Most egregious is the synthesis of the HaloTag ligand of PA-JF_{646}, which requires 17 steps with an overall yield of 0.5% (Figure S1b).[35] Unfortunately, recently described synthetic approaches for other, less bright SiRh dyes using acid-mediated chemistry[46,65] are not amenable to the JF dyes due to the instability of azetidines under these harsh conditions.

We considered whether an alternative synthetic strategy might allow for easier access to a wider variety of SiFl and SiRh dyes. Two complementary approaches to these compounds are shown in Figure 1b. Route 1 depicts the established methodology,[15,17,43,44,46,55] where a metalated aryl species (**5**) is added to a Si-anthrone (**4**) to install the pendant aryl ring of the SiFl (**8**) or SiRh (**9**). This route, however, presents a mismatch between reacting partners; the ketone electrophile is electron-rich due to the heteroatom substituents (Y), and the arylmetal nucleophile is routinely electron-poor owing to the ester functionality necessary to install the requisite *ortho*-carboxy group of the dye. This mismatch limits the use of milder arylmetal reagents such as Grignard reagents—particularly when Y = NR^2R^3—and often requires a more forcing aryllithium protocol that is incompatible with many functional groups and requires the use of complex protection strategies. Furthermore, the syntheses of the Si-anthrones are in some cases rather long and poorly scalable, as evidenced by the preparation of the ketone (**4**, Y = OTBS; 7 steps, 10% yield) necessary to prepare SiFl.[43,66]

Inspired by the classic Friedel−Crafts synthesis of fluoresceins and rhodamines,[5] we considered an alternative, synthon-reversed route for SiFl and SiRh dyes (Route 2, Figure 1b). In this strategy, the upper portion of the dye would be derived from an electron-rich bis(arylmetal) intermediate **6**, which we anticipated could add twice to an ester or anhydride (**7**) to form the central C−C bonds of the dye (**8** or **9**) in an electronically matched reaction. Moreover, we aimed to prepare **6** from the corresponding dibromides, which are substantially easier to access than the Si-anthrone intermediates. Here, we describe this strategy as a general method for the synthesis of SiFl and SiRh fluorophores. Facile preparation of bis(5-alkoxy-2-bromophenyl)silanes allowed for the optimization of a three-step protocol for direct synthesis of Si-fluoresceins: Li/Br-exchange, transmetalation to magnesium, and electrophile addition. The concise nature of this protocol allowed synthesis of new SiFl derivatives where the pK_a is modulated through incorporation of fluorine substituents. We then extended this approach to the synthesis of SiRh dyes, where the analogous reaction of bis(5-amino-2-bromophenyl)silanes afforded direct access to a variety of novel JF_{646} derivatives as well as other SiRh, Si-rosamine, and Si-pyronine derivatives. This rapid, divergent strategy allowed for brief, 3−4 step syntheses of new Si-containing dyes, yielded new stains and labels for cellular imaging, and could be extended to prepare novel derivatives of classic oxygen-containing rhodamines.

RESULTS AND DISCUSSION

Synthesis of Si-Fluoresceins. We previously reported and characterized SiFl (**1**) during the synthesis of SiRh dyes such as JF_{646}.[15] Under basic conditions (0.1 N NaOH), SiFl exhibited the expected red-shift in spectra (λ_{max} = 579 nm, λ_{em} = 599 nm), as well as a high extinction coefficient (ε = 93 000 M^{-1} cm^{-1}) and quantum yield (Φ = 0.53). This dye also displayed interesting pH sensitivity, undergoing a cooperative transition from a colored, fluorescent form to a nonfluorescent lactone form with a Hill coefficient (h) value of 1.69. This colored → colorless transition has also been observed in carbon-substituted fluorescein derivatives[40,41] and highlights how this silicon modification to the fluorescein structure alters the open−closed equilibrium. Although these characteristics would appear to make SiFl well-suited for application as a pH sensor or fluorogenic scaffold, the pK_a = 8.27 is substantially higher than physiological pH (7.4), rendering the molecule largely colorless in biological samples and limiting its utility for imaging. We therefore sought to use this new bis(arylmetal) strategy to not only access SiFl (**1**) more efficiently, but also to extend the usefulness of this dye through incorporation of fluorine substituents. Fluorination, most commonly at the 2′ and 7′ positions, is a well-established technique for decreasing the pK_a of fluoresceins, as has been demonstrated with Oregon Green (2′,7′-difluorofluorescein)[67] and Virginia Orange (2′,7′-difluorocarbofluorescein).[41] Nagano recently described 4′,5′-difluoro-SiFl,[49] which demonstrated a pK_a close to physiological pH, but we sought to further reduce the pK_a to provide analogues that would be fully open and fluorescent under physiological conditions. For this reason, we targeted derivatives with between two and six fluorine substituents at positions throughout the SiFl structure.

We began our exploration of this synthetic approach to the SiFl scaffold by preparing the necessary bis(5-alkoxy-2-bromophenyl)silane intermediates **12a−c** (Scheme 1, Supporting Information). Commercially available 3-bromophenols were protected as methoxymethyl (MOM) ethers to give **10a−c**, which underwent Li/Br-exchange with *n*-BuLi and addition to dichlorodimethylsilane to afford silanes **11a−c**. For the nonfluorinated compound **11a**, regioselective *para*-bromination was easily achieved with *N*-bromosuccinimide (NBS) in dimethylformamide (DMF) to provide the key intermediate

DOI: 10.1021/acscentsci.7b00247
ACS Cent. Sci. 2017, 3, 975−985

Scheme 1. Bis(5-methoxymethoxy-2-bromophenyl)silane Syntheses

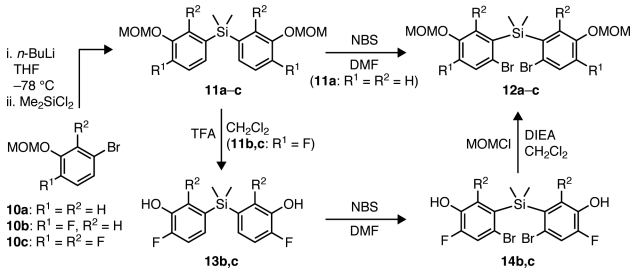

12a in nearly quantitative yield (94%). The less nucleophilic silanes (**11b,c**) could not be brominated with NBS or Br_2 unless heating was applied, which decreased regioselectivity and yields. We found that temporary removal of the MOM groups to give diphenols **13b,c** provided substrates that were much more amenable to NBS bromination. Simple reprotection of **14b,c** with MOMCl then afforded the necessary fluorinated bis(5-alkoxy-2-bromophenyl)silanes (**12b,c**).

With these dibromides in hand, we then implemented the Li/Br-exchange and addition strategy to prepare a set of SiFl analogues (Figure 2a). Using **12a** as the proof-of-concept substrate, a small set of reaction conditions were screened (selected examples in Table S1). Although *t*-BuLi-mediated Li/Br-exchange and immediate addition of the phthalic anhydride electrophile (**15**) gave reasonable results for the preparation of protected SiFl **18** (40% yield), we found that intervening transmetalation to magnesium via addition of $MgBr_2{\cdot}OEt_2$ provided higher yields and demonstrated greater functional group tolerance for other dibromide/electrophile combinations (vide infra). Dibromide **12a** underwent this three-step, one-pot procedure with phthalic anhydride (**15**) to provide MOM_2-SiFl (**18**) in 60% yield; routine MOM deprotection of **18** with TFA to furnish SiFl (**1**) was quantitative. Overall, this synthetic route provided **1** in five steps and 48% overall yield from 3-bromophenol, which represents an 8-fold improvement in yield and four fewer steps when compared to our previous synthesis.[15] The fluorinated dibromides **12b** and **12c** were similarly reacted with phthalic anhydride to give 2′,7′-difluoro-SiFl (**24**) and 2′,4′,5′,7′-tetrafluoro-SiFl (**25**) in good two-step yields (54–55%).

This strategy could also be used to incorporate useful functionality on the pendant phenyl ring of the dyes. To explore how fluorination of this bottom ring might impact the pH sensitivity of SiFl, dibromides **12a,b** were subjected to the same three-step reaction (Li/Br-exchange, Mg-transmetalation, electrophile addition) with tetrafluorophthalic anhydride (**16**). This allowed easy access to **21** and **22** in reasonable yield (42–46%), which upon clean removal of the MOM groups, afforded 4,5,6,7-tetrafluoro-SiFl (**26**) and the highly substituted 2′,4,5,6,7,7′-hexafluoro-SiFl (**27**). Importantly, transmetalation to magnesium was essential to achieving acceptable yields with **16**. Direct reaction of the bis-aryllithium intermediates with tetrafluorophthalic anhydride provided low yields and multiple side products, demonstrating the importance of moderating the reactivity of the bis(arylmetal)silane species. Another desirable functionality is a 5- or 6-carboxyl group on the lower aryl ring, as such a handle for bioconjugation is often crucial for the application of xanthene-based dyes. Because metalation of **12a** and addition to protected 4-carboxyphthalic anhydrides provided inseparable mixtures of regioisomers, we instead

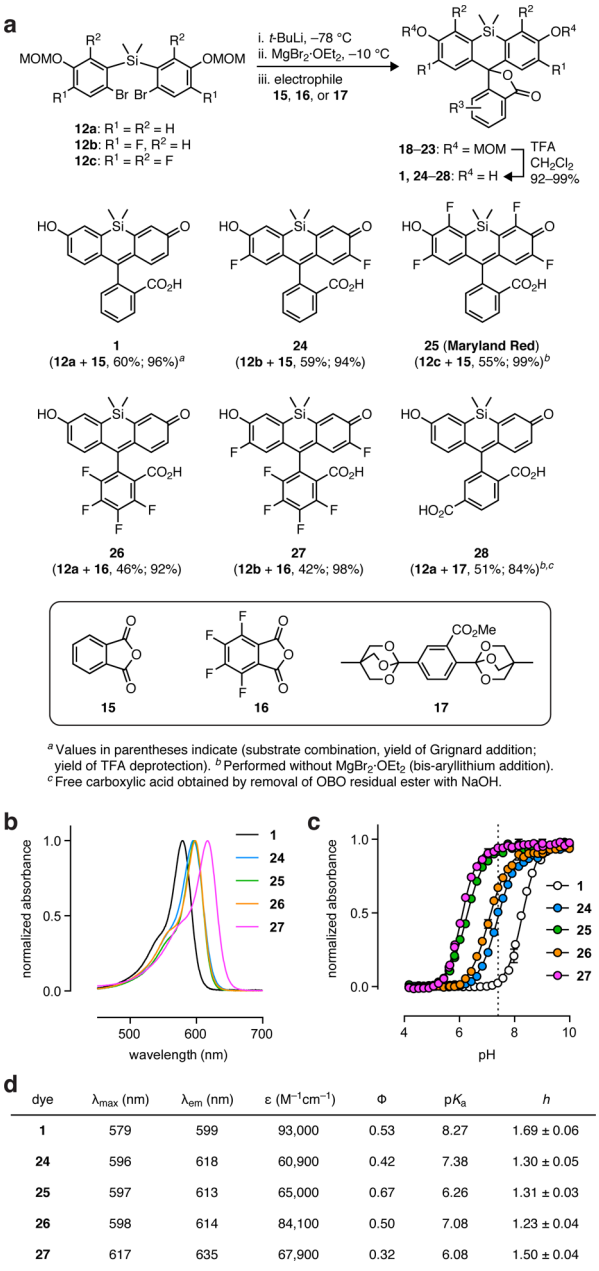

d

dye	λ_{max} (nm)	λ_{em} (nm)	ε ($M^{-1}cm^{-1}$)	Φ	pK_a	*h*
1	579	599	93,000	0.53	8.27	1.69 ± 0.06
24	596	618	60,900	0.42	7.38	1.30 ± 0.05
25	597	613	65,000	0.67	6.26	1.31 ± 0.03
26	598	614	84,100	0.50	7.08	1.23 ± 0.04
27	617	635	67,900	0.32	6.08	1.50 ± 0.04

Figure 2. Synthesis and properties of Si-fluoresceins. (a) Synthesis of Si-fluoresceins **1** and **24–28** via Li/Br exchange, transmetalation to magnesium, electrophile addition, and MOM deprotection. (b) Normalized absorbance spectra of **1** and **24–27** in 0.1 N NaOH. (c) Normalized absorbance at λ_{max} versus pH for **1** and **24–27**. Dashed line indicates pH 7.4. Error bars show standard error (SE; n = 2). (d) Spectroscopic data for Si-fluoresceins **1** and **24–27**.

chose to use an orthoester (4-methyl-2,6,7-trioxa-bicyclo[2.2.2]octan-1-yl, OBO) protecting group strategy, which we established previously for photoactivatable SiRh derivatives.[35] Convenient access to 6-carboxy-Si-fluorescein (**28**) was thereby achieved through Li/Br-exchange of **12a** and addition to bis-OBO-protected methyl 2,5-dicarboxy-benzoate **17** (51% yield), followed by removal of the MOM and OBO protecting groups (84% yield).

Spectral Properties of Si-Fluoresceins. The spectral properties of the new SiFl derivatives **24–27** were then evaluated and compared to those of the parent SiFl (**1**; Figure 2b–d). When the absorbance and fluorescence emission

DOI: 10.1021/acscentsci.7b00247
ACS Cent. Sci. 2017, 3, 975–985

Table 1. Synthesis of Si-Rhodamines, Si-Rosamines, and Si-Pyronines from Bis(5-amino-2-bromophenyl)silanes

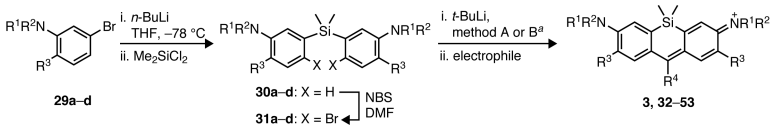

dibromide	NR^1R^2	R^3	method[a]	electrophile	R^4	yield (%)	dye
31a		H	A			55	**3**
31b		F	A			44	**32**
31c	NMe_2	H	A			66	**33**
31d		H	A			55	**34**
31a		H	A	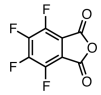	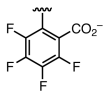	51	**35**
31b		F	A			40	**36**
31c	NMe_2	H	A			52	**37**
31d		H	A			47	**38**
31a		H	A	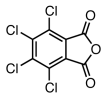	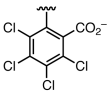	44	**39**
31a		H	A		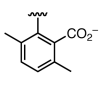	63	**40**
31a		H	A		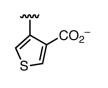	30	**41**
31a		H	B		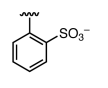	32	**42**
31a		H	A			9	**43**

dibromide	NR^1R^2	R^3	method[a]	electrophile	R^4	yield (%)	dye
31a		H	B			75	**44**
31a		H	B			88	**45**
31a		H	B			4	**46**
31a		H	B	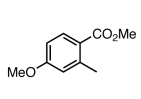		58	**47**
31a		H	B			78[b]	**48**
31a		H	B			65	**49**
31a		H	B	HCO_2Me		50	**50**
31a		H	B			62[c]	**51**
31a		H	B			49[c]	**52**
31c	NMe_2	H	B			53[d]	**53**

[a]Method A: *t*-BuLi (4.4 equiv), THF, −78 °C to −10 °C, then $MgBr_2{\cdot}OEt_2$, −10 °C, then electrophile, −10 °C to rt; Method B: *t*-BuLi (4.4 equiv), THF, −78 °C to −20 °C, then electrophile, −20 °C to rt. [b]Two-step yield that includes MOM deprotection with TFA. [c]Two-step yield that includes removal of OBO residual ester via hydrolysis with NaOH. [d]Two-step yield that includes oxazoline deprotection with aqueous HCl.

spectra were recorded, it was found that the presence of two or four fluorine substituents (**24**–**26**) resulted in a 15–20 nm bathochromic shift in λ_{max} and λ_{em}, regardless of the location of the F atoms (Figure 2b,d); the hexafluoro-substituted **27** showed a further ∼20 nm red shift. The extinction coefficient of **26** at high pH (0.1 N NaOH; ε = 84 100 M^{-1} cm^{-1}) was similar to that of SiFl (ε = 93 000 M^{-1} cm^{-1}); the other fluorinated derivative (**24**, **25**, and **27**) displayed decreased values for ε (60 900–67 900 M^{-1} cm^{-1}). Curiously, **25** showed a quantum yield (Φ = 0.67) significantly higher than SiFl (Φ = 0.52), whereas **26** (Φ = 0.50) was similar to the parent dye and **24** and **27** (Φ = 0.42, 0.32) were lower. Most importantly, fluorination of SiFl had a pronounced, additive effect on pH sensitivity, with more fluorine substituents resulting in larger decreases in pK_a (Figure 2c,d). The incorporation of two fluorines (**24**) lowered the pK_a of SiFl (8.27) by nearly one unit to 7.38. Placing four fluorine substituents on the bottom ring (**26**) provided a dye with a pK_a = 7.08, and the effect was even larger when the four fluorines were incorporated into the top dibenzosiline portion of the dye (**25**, pK_a = 6.26). Not surprisingly, hexafluoro-Si-fluorescein **27** showed the lowest pK_a = 6.08. As a result, both **25** and **27** were fully deprotonated and highly fluorescent at physiological pH (7.4, Figure 2c). Because of its high quantum yield, convenient spectra, and ideal pK_a for many biological applications, we named **25** "Maryland Red" (in the fashion of "Virginia Orange"[41] and "Oregon Green"[67]). All the Si-fluoresceins were colorless and non-fluorescent at low pH and exhibited Hill coefficients above 1 (h = 1.23–1.69), indicating that they maintain the cooperativity of protonation and shifted open–closed equilibrium that we previously observed for the carbofluoresceins.[40,41] These properties demonstrate that the fluorinated Si-fluoresceins—particularly Maryland Red (**25**) and the hexafluoro derivative **27**—would serve as desirable, further red-shifted scaffolds for pH sensors or fluorogenic molecules, including single- or dual-input logic gates[41] and reaction-based indicators.[23]

DOI: 10.1021/acscentsci.7b00247
ACS Cent. Sci. 2017, 3, 975–985

Synthesis of Si-Rhodamines. The substantially shorter synthetic route to SiFl derivatives inherently provided us with one avenue to quickly prepare JF_{646} derivatives through Pd-catalyzed C−N cross-coupling of SiFl ditriflate (Figure 1a).[15] In addition, we explored whether the same strategy could be applied to directly access SiRh dyes from the metalation of analogous bis(5-amino-2-bromophenyl)silanes. We sought to not only access JF_{646} itself but also demonstrate the generality of a bis-metalation/addition route to access a variety of SiRh dyes with diverse substitution patterns, both on the aniline nitrogens and elsewhere on the scaffold. We began by preparing a small set of bis(5-amino-2-bromophenyl)silanes that included the necessary precursors for the synthesis of bis(azetidinyl)-SiRh dyes (**31a**,**b**, Table 1) and those with other amino substituents (**31c**,**d**). These substrates were easily prepared in 2−3 steps from commercially available starting materials, as shown in Table 1. Lithium-bromide exchange of 3-bromoanilines **29a**−**d** with *n*-BuLi and addition to dichlorodimethylsilane yielded bis(3-aminophenyl)silanes **30a**−**d**. Regioselective *para*-bromination was achieved as before with NBS in DMF to afford dibromides **31a**−**d** in good to excellent overall yield (Supporting Information).

Beginning with **31a** and phthalic anhydride, we once again performed a brief screen of reaction conditions for the exchange/transmetalation/addition reaction sequence (Table S2). As before, Li/Br-exchange with excess *t*-BuLi, transmetalation with $MgBr_2{\cdot}OEt_2$, and subsequent electrophile addition provided the highest yields of the Si-rhodamine products. Slow addition of the anhydride at −10 °C was critical to avoid the formation of side products resulting from the addition of one bis(aryl Grignard) species to two molecules of anhydride. We note that attempts to directly form the arylmagnesium species from the dibromide with several Grignard reagents—including *i*-PrMgCl·LiCl and *i*-$PrBu_2MgLi$—were sluggish and gave poor yields. Application of this protocol to **31a** and phthalic anhydride afforded JF_{646} (**3**) in 55% yield (Table 1). When compared to our previous synthesis of JF_{646} (11 steps, 4.6% yield),[15] this four-step sequence represents a nearly 10-fold improvement in yield (44% overall yield from 3-bromoiodobenzene). Each of the four dibromides (**31a**−**d**) was well-tolerated in combination with phthalic or tetrafluorophthalic anhydride, providing access to 2′,7′-difluoro-JF_{646} (**32**), Si-tetramethylrhodamine (SiTMR, **33**),[46] and bis(azepanyl)-SiRh (**34**), as well as their 4,5,6,7-tetrafluorinated analogues **35**−**38**, in moderate to good yield (40−66%). We note that previous efforts to synthesize 4,5,6,7-tetrafluoro-SiTMR (**37**) through an aryllithium addition to a Si-anthrone were unsuccessful.[55] The relatively facile syntheses of the tetrafluorinated congeners of JF_{646} and SiTMR (**35** and **37**) demonstrate the complementarity of this strategy and the ability to assemble previously inaccessible SiRh derivatives. We could also use this approach with another reactant bearing an electrophilic, halogenated aryl system—tetrachlorophthalic anhydride—which afforded 4,5,6,7-tetrachloro-JF_{646} (**39**, 44% yield). In this case, transmetalation to the magnesium adduct was essential, as direct reaction of the bis-aryllithium species with tetrachlorophthalic anhydride afforded only trace product. The reaction scope also encompassed a more sterically encumbered anhydride (3,6-dimethylphthalic anhydride) and a heterocyclic anhydride (3,4-thiophenedicarboxylic anhydride) to yield **40** (63%) and **41** (30%), respectively. Sulfo-JF_{646} (**42**)—which bears an *ortho*-sulfonate on the bottom ring instead of the typical *o*-carboxylate—was likewise synthesized when 2-sulfobenzoic acid cyclic anhydride was used as the electrophile. In this case, higher yields were obtained by using the bis-aryllithium directly, without the $MgBr_2{\cdot}OEt_2$ additive. Finally, succinic anhydride was a modest substrate for this reaction, giving a low yield (9%) but nonetheless providing access to succinyl-JF_{646} ("S-JF_{646}", **43**), the first silicon analogue of succinyl-fluoresceins or -rhodamines.[68]

As demonstrated by the synthesis of 6-carboxy-SiFl (**28**, Figure 2a), methyl esters are also suitable electrophilic substrates for the dibromide exchange/addition reaction. We briefly explored the scope of methyl benzoates and related esters as a means of accessing various Si-rosamines and Si-pyronines (Table 1, right column). When using esters as electrophiles, direct addition of the bis-aryllithium species to the esters consistently provided higher yields of the Si-xanthene products than transmetalation to magnesium and addition of the bis(aryl Grignard). Reaction of **31a** with *t*-BuLi and several methyl benzoates provided Si-rosamines **44**, **45**, and **47**−**49** in good to excellent yield (58−88%); these included analogues containing an *ortho*-hydroxyl substituent (**48**) and a pyridine (**49**). Not surprisingly, the highly hindered methyl 2,6-dimethylbenzoate provided only a modest amount of the corresponding Si-rosamine (**46**, 4%). Small, simple, non-benzoate esters—methyl formate and a monoprotected ethyl oxalate—also underwent reaction with the bis-aryllithium of **31a** to yield the compact Si-pyronine dyes **50** and **51**.[42] As with SiFl derivatives, the presence of a carboxyl handle on SiRh dyes is often critical for biological utility. We expected that 6-carboxy-JF_{646} would be accessible by employing the same bis-OBO-protected methyl 2,5-dicarboxybenzoate (**17**) used previously (Figure 2a, Table 1). Li/Br-exchange of **31a**, addition of **17**, and deprotection using atypical hydrolysis conditions (Supporting Information) afforded the valuable 6-carboxy-JF_{646} (**52**) in 49% yield, constituting a succinct route to this useful fluorophore (five steps, 39% overall yield). Likewise, 6-carboxy-SiTMR (**53**) was prepared in a straightforward fashion from **31c** and a bis-oxazoline[46] methyl benzoate, affording a 53% yield after oxazoline removal by HCl. We note the oxazoline protecting group is not compatible with the azetidinyl rhodamine system due to the harsh deprotection conditions (6 N HCl, 80 °C, 12 h) required for its removal.

Spectral Properties of Si-Rhodamines. Having synthesized a substantial panel of SiRh dyes and related fluorophores (**32**, **34**−**53**), we evaluated their spectral properties and compared them to existing dyes such as JF_{646} (**3**) and SiTMR (**33**).[15,46] The data for selected compounds are given in Table 2; a comprehensive listing of all spectral properties can be found in Table S3 (Supporting Information). As previously described, SiRh dyes typically exhibit low visible absorbance in aqueous solution due to a shift in the lactone−zwitterion equilibrium to the closed, colorless, lactone form. For example, JF_{646} (**3**) exhibits $\lambda_{max}/\lambda_{em}$ = 646 nm/664 nm and a quantum yield (Φ) of 0.54, but its extinction coefficient in water is low (ε_{water} = 5600 M^{-1} cm^{-1}). To further compare the various Si-rhodamines, we measured the visible absorbance of the dyes in acidic media (ethanol or 2,2,2-trifluoroethanol with 0.1% v/v TFA), which shifts xanthene dyes to the zwitterionic (open) form and provides a reasonable estimate of a maximal extinction coefficient (ε_{max}).[69,70] For example, the tetrafluorinated analogue of JF_{646} (**35**) exhibited a ∼20 nm red shift ($\lambda_{max}/\lambda_{em}$ = 669 nm/682 nm), but a somewhat lower quantum yield (Φ = 0.37) compared to JF_{646}. More importantly, **35** was highly absorbing in aqueous solution and exhibited an

DOI: 10.1021/acscentsci.7b00247
ACS Cent. Sci. 2017, 3, 975−985

Table 2. Spectroscopic Data for Selected Si-Rhodamines, Si-Rosamines, and Si-Pyronines[a]

	dye	λ_{max} (nm)	λ_{em} (nm)	ε_{water} ($M^{-1}cm^{-1}$)	ε_{max} ($M^{-1}cm^{-1}$)[a]	Φ
azetidinyl SiRh	**3**	646	664	5,600	152,000	0.54
	35	669	682	112,000	116,000	0.37
	39	674	685	9,870	84,500	0.14
	41	650	667	113,000	149,000	0.40
	42	654	670	124,000	139,000	0.51
	43	652	668	21,200	126,000	0.25
SiTMR	**33**	643	662	28,200	141,000	0.41
	37	667	682	132,000	139,000	0.31
azepanyl SiRh	**34**	657	674	2,200	185,000	–[b]
	38	683	698	15,500	215,000	0.10
Si-rosamine and Si-pyronine	**44**	648	662	116,000	–	0.20
	45	649	663	118,000	–	0.47
	48	651	666	136,000	–	0.48
	50	636	649	97,100	–	0.62
	51	641	657	120,000	–	0.26

[a]All properties (except ε_{max}) taken in 10 mM HEPES pH 7.3. [b]Extinction coefficient as measured in acidic alcohol (ethanol or 2,2,2-trifluoroethanol with 0.1% v/v TFA). [c]Quantum yield could not be determined due to low aqueous solubility and predominance of the closed form in water.

extinction coefficient (ε_{water} = 112 000 M^{-1} cm^{-1}) nearly the same as ε_{max} (116 000 M^{-1} cm^{-1}), likely due to a significant shift in the open−closed equilibrium. On the basis of its λ_{max}, we named this fluorophore "Janelia Fluor 669" (JF_{669}). Tetrachlorination of the bottom ring had a much smaller effect on the lactone−zwitterion equilibrium, producing a dye (**39**) with a lower absorbance in water (ε_{water} = 9870 M^{-1} cm^{-1}) and a substantially decreased Φ = 0.14, albeit with a larger red-shift in wavelengths ($\lambda_{max}/\lambda_{em}$ = 674 nm/685 nm). The effect of 4,5,6,7-tetrafluorination was consistent across different Si-rhodamines. Whereas SiTMR (**33**) had a modest ε_{water} = 28 200 M^{-1} cm^{-1} compared to its ε_{max} = 141 000 M^{-1} cm^{-1}, tetrafluoro analogue **37** was strongly shifted to the open form in solution (ε_{water} = 132 000 M^{-1} cm^{-1}, ε_{max} = 139 000 M^{-1} cm^{-1}), with similar 20−24 nm bathochromic shifts for λ_{max} (667 nm) and λ_{em} (682 nm). The same result was observed for the two bis(azepanyl)-Si-rhodamines **34** and **38**. The JF_{646} analogues with 2′,7′-difluoro substitution (**32**, **36**) and 4,7-dimethyl compound **40** were poorly soluble and strongly shifted to the closed form in most solvents, resulting in extremely low or unmeasurable ε_{water} values (Table S3).

Modifications beyond halogenation could significantly alter the spectral properties and open−closed equilibrium of **3**. Replacement of the pendant phenyl ring with a thiophene provided a thienyl-JF_{646} (**41**) with wavelengths similar to JF_{646} ($\lambda_{max}/\lambda_{em}$ = 650 nm/667 nm) and a slightly lower quantum yield (Φ = 0.40). Its equilibrium, however, was strongly shifted to the zwitterionic form, as demonstrated by a strong aqueous absorbance (ε_{water} = 113 000 M^{-1} cm^{-1}) similar to ε_{max} (149 000 M^{-1} cm^{-1}). A similarly dramatic effect was seen with the *ortho*-sulfonate analogue (sulfo-JF_{646}, **42**), the azetidinyl analogue of Berkeley Red,[52] which preserved the higher quantum yield (Φ = 0.51) of JF_{646} but was almost exclusively open in water (ε_{water} = 124 000 M^{-1} cm^{-1}, ε_{max} = 139 000 M^{-1} cm^{-1}). The unusual S-JF_{646} (**43**), which contains an ethylene linker in place of the aryl ring, was more akin to JF_{646}; it displayed λ_{max} = 652 nm, λ_{em} = 668 nm, and ε_{water} = 21 200 M^{-1} cm^{-1} but showed a lower quantum yield of Φ = 0.25.

The Si-rosamines (**44**−**49**) and Si-pyronines (**50**, **51**) do not exhibit the open−closed equilibrium, making their spectral characterization more straightforward (Table 2, Table S3). The Si-rosamines all showed λ_{max} and λ_{em} values near 650 and 664 nm, respectively, although the pyridine **49** was slightly red-shifted ($\lambda_{max}/\lambda_{em}$ = 656 nm/670 nm). The extinction coefficients ranged from 89 600 M^{-1} cm^{-1} (dimethyl analogue **46**) to 136 000 M^{-1} cm^{-1} (*o*-hydroxyl analogue **48**), with most derivatives clustered near 115 000 M^{-1} cm^{-1}. Unsubstituted phenyl derivative **44** displayed a lower quantum yield (Φ = 0.20) than the other Si-rosamines. Installation of one *ortho*-substituent was sufficient to achieve a significant recovery in quantum yield with the other Si-rosamines (**45**−**49**) all exhibiting Φ ≈ 0.50. The small, compact Si-pyronine **50**—which entirely lacks a 9-substituent—showed a surprisingly high quantum yield for a Si-xanthene dye (Φ = 0.62), with blue-shifted wavelengths ($\lambda_{max}/\lambda_{em}$ = 636 nm/649 nm) relative to the other Si-dyes and ε = 97 100 M^{-1} cm^{-1}. Dye **50** is also 5-fold brighter than the tetramethyl-Si-pyronine—the original Si-xanthene dye reported by Fu (ε = 64 200 M^{-1} cm^{-1}, Φ = 0.18).[42] The addition of a carboxyl group in **51**—a potential functional handle—improved absorptivity (ε = 120 000 M^{-1} cm^{-1}) but decreased quantum yield (Φ = 0.26).

Altogether, this collection of fluorophores (particularly **3**, **32**−**43**) demonstrates several techniques for structural modification that significantly alter the open−closed equilibrium of Si-rhodamines. Although the propensity of Si-rhodamines like SiTMR and JF_{646} to close in an aqueous environment can be exploited to prepare fluorogenic labels,[15,46] it also limits their utility in other contexts. The modifications to the pendant aryl ring that stabilize the fluorescent, zwitterionic form—sulfonation (**42**), use of smaller heterocycles (**41**), or fluorination (**35**, **37**, **38**)—should allow for an expansion of the utility of Si-rhodamines as more general cellular stains, indicators, and labels that retain the brightness and red-shifted spectra of the Si-xanthene fluorophores.

Synthesis of Fluorinated Classic Rhodamines. Having established the bis(2-bromophenyl)silane route as a general strategy for the synthesis of SiFl and SiRh dyes, we considered whether this protocol might also be useful for the preparation of classic, oxygen-containing rhodamines. Although reaction of resorcinol-derived aryl Grignards with methylbenzoates has been employed to prepare fluorone dyes,[71,72] fluoresceins and rhodamines are most commonly prepared via the acid-mediated condensation of resorcinols or 3-aminophenols with anhydrides.[5] Unfortunately, the harsh conditions necessary for this synthesis severely limit the type of chemical functionality that can be incorporated into the rhodamine structure. For example, the azetidinyl rhodamine based Janelia Fluor dyes cannot be prepared via this route due to the propensity for the four-membered rings to open under strong acid. The Pd-catalyzed cross-coupling of fluorescein ditriflates with azetidines was instead used to access dyes like JF_{549}.[15] The scope of the cross-coupling is quite broad, but rhodamines fluorinated on the xanthene ring (**58**, Scheme 2), the pendant phenyl ring (**59**) or both (**60**) proved elusive due to the reactivity of the fluorinated fluorescein ditriflates under cross-coupling conditions.

As demonstrated with fluorinated SiFl (Figure 2) and SiRh (Table 1) derivatives, the dibromide approach is compatible with fluorinated starting materials. We therefore applied this synthetic route to synthesize fluorinated rhodamine dyes **58**−

DOI: 10.1021/acscentsci.7b00247
ACS Cent. Sci. 2017, 3, 975−985

Scheme 2. Extension of the Dibromide Approach to Fluorinated Rhodamines

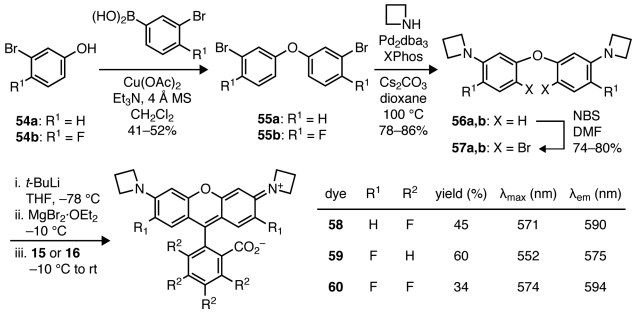

dye	R^1	R^2	yield (%)	λ_{max} (nm)	λ_{em} (nm)
58	H	F	45	571	590
59	F	H	60	552	575
60	F	F	34	574	594

60 in only four steps each (Scheme 2). The necessary brominated diphenyl ethers **57a,b** were prepared by Chan–Lam coupling[73−75] of 3-bromophenols **54a,b** and 3-bromophenyl-boronic acids, followed by cross-coupling with azetidine and consistently clean NBS bromination.[76] The same *t*-BuLi/$MgBr_2$·OEt_2 protocol and addition to phthalic anhydride (**15**) or tetrafluorophthalic anhydride (**16**) provided the fluorinated rhodamines **58**–**60** in moderate yields (34–60%). The new 4,5,6,7-tetrafluororhodamine **65**, which we named "Janelia Fluor 571" (JF_{571}), exhibited the expected ~20 nm shift in spectral properties ($\lambda_{max}/\lambda_{em}$ = 571 nm/590 nm, Scheme 2) relative to JF_{549} ($\lambda_{max}/\lambda_{em}$ = 549 nm/571 nm).[15] Fluorination at the 2′ and 7′ positions (**59**, JF_{552}) elicits a smaller change in spectral properties ($\lambda_{max}/\lambda_{em}$ = 552 nm/575 nm) and the 2′,4,5,6,7,7′ -hexafluororhodamine (**60**, JF_{574}) shows an additive shift in spectral properties ($\lambda_{max}/\lambda_{em}$ = 574 nm/594 nm). All the fluorinated dyes maintained the high brightness of the parent JF_{549} (Table S3), establishing the utility of fluorination as a strategy to fine-tune spectral properties without adversely affecting ε or Φ. More generally, this straightforward and modular synthesis complements existing methods for the preparation of traditional rhodamines and presents multiple opportunities for the preparation of compounds beyond **58**–**60**, whether through incorporation of functionality into the simple phenyl starting materials or the attachment of different amines in the C–N cross-coupling.

Fluorinated SiRh Dyes As Biomolecular Labels. We then explored the use of selected new SiRh dyes as biomolecular labels in fluorescence imaging experiments. Previous work has demonstrated that xanthene dyes with halogenated pendant rings are facile substrates for nucleophilic aromatic substitution reactions with thiols.[9,77] This provides an alternate method for bioconjugation that can obviate the need for de novo incorporation of synthetically problematic functional handles like carboxylates, maleimides, or haloacetamides. We found that the tetrafluorinated Si-rhodamines can be derivatized in this way (Figure 3), providing another use for this structural modification beyond manipulation of spectral and chemical properties. For example, JF_{669} (**35**) can be directly reacted with the commercially available thiol-containing HaloTag ligand under mild conditions (DIEA, DMF) to afford a JF_{669}–HaloTag ligand (**61**) in a single step. The substitution reaction appeared to be highly dependent on the open–closed equilibrium; JF_{669} underwent rapid conversion to thioether product (<5 min to completion) in organic solvents, where the dye predominantly adopts the closed form. Incubation of JF_{669} with thiol in aqueous media, however, resulted in negligible product after several hours (<1% after 4 h, Figure S2). We could also append a more traditional amine-reactive handle by

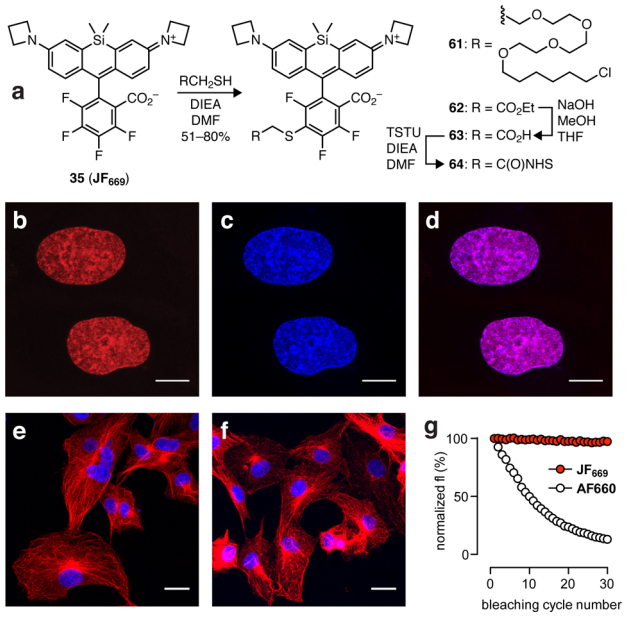

Figure 3. Cellular imaging with thioether derivatives of JF_{669}. (a) Synthesis of thioethers **61** and **64** via S_NAr of JF_{669} (**35**) with thiols. (b–d) Confocal maximum projection images of live, washed U2OS cells expressing HaloTag-H2B, incubated with JF_{669}-thio-HaloTag ligand **61** and counterstained with Hoechst 33342: (b) JF_{669}, red; (c) Hoechst 33342, blue; (d) merge. Scale bars = 10 μm. (e–f) Confocal images of fixed COS7 cells with immunolabeled microtubules (red), counterstained with Hoechst 33342 (blue): (e) JF_{669}-antibody conjugate from **64**; (f) Alexa Fluor 660-antibody conjugate. Scale bars = 20 μm. (g) Photostability of JF_{669} and AF660, as represented by the normalized decrease in fluorescence signal after repeated bleaching cycles. Performed on COS7 cells immunolabeled with dye-antibody conjugates.

reaction of JF_{669} with ethyl thioglycolate and two-step conversion of the resulting ethyl ester (**62**) via carboxylic acid **63** to the NHS ester (**64**). The thioether products exhibited spectral properties nearly identical to JF_{669} (**62**, **63**, Table S3). U2OS cells expressing a HaloTag-histone H2B protein fusion were incubated with ligand **61** and Hoechst 33342 followed by brief washing; we observed brightly labeled nuclei with excellent colocalization and low background (Figure 3b–d), demonstrating that this new label retains the cell permeability and selective labeling of JF_{646}–HaloTag ligand[15] while requiring only five synthetic steps. As an additional example of the utility of fluorinated Si-rhodamine labels, we performed immunolabeling of tubulin in fixed COS7 cells using a secondary antibody labeled with the *N*-hydroxysuccinimidyl esters of either Janelia Fluor 669 (JF_{669}–NHS, **64**) or Alexa Fluor 660 (AF660-NHS). Both dye–antibody conjugates were effective immunofluorescence labels for imaging of tubulin (Figure 3e,f). The photostabilities of the two dyes were also compared in matched conditions. Whereas the fluorescence of Alexa Fluor 660 was reduced to 13% after 30 bleaching cycles, JF_{669} displayed comparatively excellent photostability, retaining 97% fluorescence after the same number of cycles (Figure 3g). These data showcase the excellent photostability of Si-rhodamine dyes compared to other far-red fluorophore types.

A Far-Red Membrane Stain. Finally, we applied our chemistry to fine-tune a lipid probe for cellular imaging. In a previous report, we briefly described the serendipitous behavior of the bis(azepanyl)-rhodamine (**65**, "Potomac Yellow", Figure

DOI: 10.1021/acscentsci.7b00247
ACS Cent. Sci. 2017, 3, 975–985

4a) as an effective internal membrane stain for super-resolution microscopy.[8] Red-shifted congeners of Potomac Yellow would

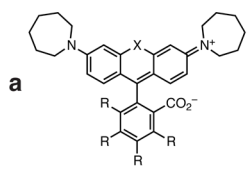

dye	X	R	λ_{max} (nm)	λ_{em} (nm)
65	O	H	560	583
66	$C(CH_3)_2$	H	618	639
34	$Si(CH_3)_2$	H	657	674
38	$Si(CH_3)_2$	F	683	698

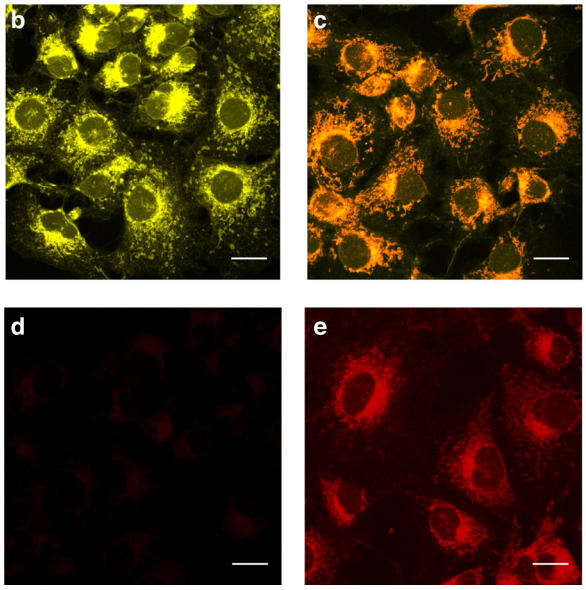

Figure 4. Bis(azepanyl)rhodamines ("Potomac" dyes) as internal membrane stains. (a) Structures and $\lambda_{max}/\lambda_{em}$ for Potomac Yellow (**65**), Potomac Orange (**66**), Si-rhodamine **34**, and Potomac Red (**38**). (b–e) Confocal microscopy of fixed COS7 cells stained with (b) Potomac Yellow (**65**), (c) Potomac Orange (**66**), (d) Si-rhodamine **34**, and (e) Potomac Red (**38**). Images d and e were taken under the same microscopy settings; scale bars = 20 μm.

be desirable for multicolor imaging experiments and those requiring deeper tissue penetration. We therefore tested the bis(azepanyl)-Si-rhodamine **34** (Table 1, Figure 4a), which exhibited the expected ~100 nm bathochromic shift compared to **65** ($\lambda_{max}/\lambda_{em}$ = 560 nm/583 nm). The bis(azepanyl)-carborhodamine **66** was also synthesized (Figure 4a, Supporting Information), as it was expected to exhibit spectra intermediate to those of **65** and **34**.[40] Spectroscopic evaluation confirmed the anticipated wavelength shifts, with **66** exhibiting $\lambda_{max}/\lambda_{em}$ = 618 nm/639 nm and **34** showing $\lambda_{max}/\lambda_{em}$ = 657 nm/674 nm (Table 2). When **65**, **66**, and **34** were compared by staining fixed COS7 cells, the rhodamine and carborhodamine analogues (**65** and **66**) displayed similarly excellent membrane staining and high fluorescence (Figure 4b,c). However, the azepane-substituted Si-rhodamine **34** showed relatively low fluorescence intensity even under high excitation laser power (Figure 4d). We attributed this to the predominance of the closed form of **34** in solution, which suggested that structural modification to shift the equilibrium to the open form would likely improve its performance as a membrane stain. We therefore tested tetrafluorinated SiRh analogue **38** based on its 7-fold higher ε_{water} (15 500 M^{-1} cm^{-1}) relative to **34** (ε_{water} = 2200 M^{-1} cm^{-1}; Tables 1 and 2). Although dimmer than **65** and **66** due to its relatively low ε_{water} value and suboptimal excitation on the microscope (633 nm), compound **38** demonstrated superior staining of COS7 cell internal membranes compared to Si-rhodamine **34** (Figure 4e). Because of its far-red wavelengths and broad potential utility as a cell-permeable stain, we named **38** "Potomac Red" (à la Nile Red[78]). The carborhodamine analogue **66** was likewise christened "Potomac Orange". These data demonstrate the value of modulating both the nitrogen substituents and pendant phenyl ring of rhodamine dyes to optimize imaging probes.

CONCLUSIONS

The xanthene dyes are ubiquitous throughout biological imaging. The silicon-containing analogues, Si-fluoresceins and Si-rhodamines, have attracted considerable interest due to their red-shifted spectra, excellent brightness, and high photostability. These properties, along with the unique shifted open–closed equilibrium, make them valuable scaffolds for fluorogenic probes and cell-permeable labels. Nevertheless, synthetic challenges have stymied the advancement and improvement of this dye type, particularly with SiRh fluorophores. Here, we have described a new, general strategy for the efficient preparation of SiFl and SiRh from simple dibromide intermediates. By reversing the synthons of the typical Si-xanthene synthesis (Figure 1), we developed an electronically matched protocol where the metal/bromide exchange of bis(2-bromophenyl)silanes is followed by double addition to anhydrides and esters, affording SiFl and SiRh dyes in fewer synthetic steps and greater overall yields. We explored modulation of the reactivity of the initial bis-aryllithium intermediate by transmetalation to magnesium. Direct reaction of the aryllithium species proved better with electron-poor dibromides (e.g., **12c**, Figure 2) or with simple ester electrophiles. The $MgBr_2{\cdot}OEt_2$ additive resulted in higher yields with anhydride electrophiles, especially halogenated phthalic anhydrides. As a proof-of-concept, we first applied this approach to SiFl (**1**), achieving a concise (five-step) and high-yielding (48%) synthesis. Incorporation of fluorines into the requisite bis(5-alkoxy-2-bromophenyl)silanes and/or the anhydride electrophile allowed for quick access to several fluorinated derivatives of SiFl (**24**–**27**, Figure 2). Higher degrees of fluorination resulted in larger reductions in pK_a relative to the unsubstituted SiFl and provided new scaffolds—such as Maryland Red (2′,4′,5′,7′-tetrafluoro-SiFl, **25**)—with improved properties for use as high-contrast, biologically useful fluorogenic probes and pH sensors.

This synthetic approach could be extended to SiRh-type dyes with broad scope (Table 1) and further applied to synthesize new fluorinated derivatives of classic rhodamines (Scheme 2). Metalation of bis(5-amino-2-bromophenyl)silanes and addition to functionalized anhydride and ester electrophiles furnished existing and novel Si-rhodamines, Si-rosamines, and Si-pyronines. In addition to providing a faster, more efficient route to known dyes like bis(azetidinyl)-SiRh (JF_{646}, **3**), this strategy allowed for perturbation of the spectral properties of Si-rhodamines through substitution or replacement of the bottom *ortho*-carboxyaryl ring. Sulfonated, heteroaromatic, and tetrafluorinated analogues of JF_{646} exhibited substantially improved visible absorbance in aqueous solution, due to shifts in the open–closed equilibrium (Table 2). The effect of tetrafluorination was general and also induced a convenient 25 nm red-shift in wavelengths as exemplified by the previously inaccessible 4,5,6,7-tetrafluoro-SiTMR (**37**). This modification allowed facile conjugation via fluoride-thiol substitution to yield cell-permeable JF_{669}–HaloTag ligand (**61**) and photostable antibody label JF_{669}–NHS (**64**, Figure 3). This modification

DOI: 10.1021/acscentsci.7b00247
ACS Cent. Sci. 2017, 3, 975–985

was also critical in the development of the novel membrane stain Potomac Red (**38**, Figure 4). Altogether, the modularity, scope, and divergent nature of this approach should further enable fine-tuning of the chemical and spectral properties of Si-fluoresceins, Si-rhodamines, and other xanthenoid dyes for an ever-expanding range of applications.

■ ASSOCIATED CONTENT

Supporting Information

The Supporting Information is available free of charge on the ACS Publications website at DOI: 10.1021/acscentsci.7b00247.

Methods for chemical synthesis, optical spectroscopy, and microscopy; characterization data for all new compounds; Figures S1 and S2; Tables S1−S3 (PDF)

■ AUTHOR INFORMATION

Corresponding Author

*E-mail: lavisl@janelia.hhmi.org.

ORCID

Luke D. Lavis: 0000-0002-0789-6343

Notes

The authors declare the following competing financial interest(s): J.B.G and L.D.L have filed patent applications on azetidine-substituted fluorophores.

■ ACKNOWLEDGMENTS

We thank Anthony Ayala (Janelia) for assistance in the scale-up of synthetic intermediates and Kathy Schaefer (Janelia) for assistance with cell culture. This work was supported by the Howard Hughes Medical Institute.

■ REFERENCES

(1) Baeyer, A. Ueber eine neue Klasse von Farbstoffen. *Ber. Dtsch. Chem. Ges.* **1871**, *4*, 555−558.

(2) Ceresole, M. Verfahren zur Darstellung von Farbstoffen aus der Gruppe des Meta-amidophenolphtaleïns D.R. Patent No. 44002, 1887.

(3) Lavis, L. D.; Raines, R. T. Bright ideas for chemical biology. *ACS Chem. Biol.* **2008**, *3*, 142−155.

(4) Haugland, R. P.; Spence, M. T. Z.; Johnson, I. D.; Basey, A. *The Handbook: A Guide to Fluorescent Probes and Labeling Technologies*, 10th ed.; Molecular Probes: Eugene, OR, 2005.

(5) Lavis, L. D.; Raines, R. T. Bright building blocks for chemical biology. *ACS Chem. Biol.* **2014**, *9*, 855−866.

(6) Lavis, L. D. Teaching old dyes new tricks: Biological probes built from fluoresceins and rhodamines. *Annu. Rev. Biochem.* **2017**, *86*, 825−843.

(7) Johnson, L. V.; Walsh, M. L.; Chen, L. B. Localization of mitochondria in living cells with rhodamine. *Proc. Natl. Acad. Sci. U. S. A.* **1980**, *77*, 990−994.

(8) Legant, W. R.; Shao, L.; Grimm, J. B.; Brown, T. A.; Milkie, D. E.; Avants, B. B.; Lavis, L. D.; Betzig, E. High-density three-dimensional localization microscopy across large volumes. *Nat. Methods* **2016**, *13*, 359−365.

(9) Panchuk-Voloshina, N.; Haugland, R. P.; Bishop-Stewart, J.; Bhalgat, M. K.; Millard, P. J.; Mao, F.; Leung, W.-Y.; Haugland, R. P. Alexa Dyes, a series of new fluorescent dyes that yield exceptionally bright, photostable conjugates. *J. Histochem. Cytochem.* **1999**, *47*, 1179−1188.

(10) Keppler, A.; Gendreizig, S.; Gronemeyer, T.; Pick, H.; Vogel, H.; Johnsson, K. A general method for the covalent labeling of fusion proteins with small molecules in vivo. *Nat. Biotechnol.* **2002**, *21*, 86−89.

(11) Liu, J. X.; Diwu, Z. J.; Leung, W. Y.; Lu, Y. X.; Patch, B.; Haugland, R. P. Rational design and synthesis of a novel class of highly fluorescent rhodamine dyes that have strong absorption at long wavelengths. *Tetrahedron Lett.* **2003**, *44*, 4355−4359.

(12) Los, G. V.; Encell, L. P.; McDougall, M. G.; Hartzell, D. D.; Karassina, N.; Zimprich, C.; Wood, M. G.; Learish, R.; Ohana, R. F.; Urh, M.; et al. HaloTag: A novel protein labeling technology for cell imaging and protein analysis. *ACS Chem. Biol.* **2008**, *3*, 373−382.

(13) Kolmakov, K.; Belov, V. N.; Bierwagen, J.; Ringemann, C.; Müller, V.; Eggeling, C.; Hell, S. W. Red emitting rhodamine dyes for fluorescence microscopy and nanoscopy. *Chem. - Eur. J.* **2010**, *16*, 158−166.

(14) Correa, I. R.; Baker, B.; Zhang, A. H.; Sun, L.; Provost, C. R.; Lukinavicius, G.; Reymond, L.; Johnsson, K.; Xu, M. Q. Substrates for improved live-cell fluorescence labeling of SNAP-tag. *Curr. Pharm. Des.* **2013**, *19*, 5414−5420.

(15) Grimm, J. B.; English, B. P.; Chen, J.; Slaughter, J. P.; Zhang, Z.; Revyakin, A.; Patel, R.; Macklin, J. J.; Normanno, D.; Singer, R. H.; Lionnet, T.; Lavis, L. D. A general method to improve fluorophores for live-cell and single-molecule microscopy. *Nat. Methods* **2015**, *12*, 244−250.

(16) Shieh, P.; Dien, V. T.; Beahm, B. J.; Castellano, J. M.; Wyss-Coray, T.; Bertozzi, C. R. CalFluors: A universal motif for fluorogenic azide probes across the visible spectrum. *J. Am. Chem. Soc.* **2015**, *137*, 7145−7151.

(17) Butkevich, A. N.; Belov, V. N.; Kolmakov, K.; Sokolov, V. V.; Shojaei, H.; Sidenstein, S. C.; Kamin, D.; Matthias, J.; Vlijm, R.; Engelhardt, J.; Hell, S. W. Hydroxylated fluorescent dyes for live cell labeling: synthesis, spectra and superresolution STED** microscopy. *Chem. - Eur. J.* **2017**, DOI: 10.1002/chem.201701216.

(18) Paradiso, A. M.; Tsien, R. Y.; Machen, T. E. Na+-H+ exchange in gastric glands as measured with a cytoplasmic-trapped, fluorescent pH indicator. *Proc. Natl. Acad. Sci. U. S. A.* **1984**, *81*, 7436−7440.

(19) Minta, A.; Kao, J. P.; Tsien, R. Y. Fluorescent indicators for cytosolic calcium based on rhodamine and fluorescein chromophores. *J. Biol. Chem.* **1989**, *264*, 8171−8178.

(20) Gee, K. R.; Brown, K. A.; Chen, W. N.; Bishop-Stewart, J.; Gray, D.; Johnson, I. Chemical and physiological characterization of fluo-4 Ca(2+)-indicator dyes. *Cell Calcium* **2000**, *27*, 97−106.

(21) Miller, E. W.; Lin, J. Y.; Frady, E. P.; Steinbach, P. A.; Kristan, W. B.; Tsien, R. Y. Optically monitoring voltage in neurons by photo-induced electron transfer through molecular wires. *Proc. Natl. Acad. Sci. U. S. A.* **2012**, *109*, 2114−2119.

(22) Miller, E. W.; Albers, A. E.; Pralle, A.; Isacoff, E. Y.; Chang, C. J. Boronate-based fluorescent probes for imaging cellular hydrogen peroxide. *J. Am. Chem. Soc.* **2005**, *127*, 16652−16659.

(23) Chan, J.; Dodani, S. C.; Chang, C. J. Reaction-based small-molecule fluorescent probes for chemoselective bioimaging. *Nat. Chem.* **2012**, *4*, 973−984.

(24) Rotman, B.; Zderic, J. A.; Edelstein, M. Fluorogenic substrates for β-D-galactosidases and phosphatases derived from fluorescein (3,6-dihydroxyfluoran) and its monomethylether. *Proc. Natl. Acad. Sci. U. S. A.* **1963**, *50*, 1−6.

(25) Wang, Z.-Q.; Liao, J.; Diwu, Z. *N*-DEVD-*N*′-morpholinecarbonyl-rhodamine 110: Novel caspase-3 fluorogenic substrates for cell-based apoptosis assay. *Bioorg. Med. Chem. Lett.* **2005**, *15*, 2335−2338.

(26) Lavis, L. D.; Chao, T.-Y.; Raines, R. T. Fluorogenic label for biomolecular imaging. *ACS Chem. Biol.* **2006**, *1*, 252−260.

(27) Rukavishnikov, A.; Gee, K. R.; Johnson, I.; Corry, S. Fluorogenic cephalosporin substrates for β-lactamase TEM-1. *Anal. Biochem.* **2011**, *419*, 9−16.

(28) Tian, L.; Yang, Y.; Wysocki, L. M.; Arnold, A. C.; Hu, A.; Ravichandran, B.; Sternson, S. M.; Looger, L. L.; Lavis, L. D. A selective esterase−ester pair for targeting small molecules with cellular specificity. *Proc. Natl. Acad. Sci. U. S. A.* **2012**, *109*, 4756−4761.

(29) Krafft, G. A.; Sutton, W. R.; Cummings, R. T. Photoactivable fluorophores. 3. Synthesis and photoactivation of fluorogenic difunctionalized fluoresceins. *J. Am. Chem. Soc.* **1988**, *110*, 301−303.

(30) Mitchison, T. J.; Sawin, K. E.; Theriot, J. A.; Gee, K.; Mallavarapu, A. [4] Caged fluorescent probes. *Methods Enzymol.* **1998**, *291*, 63−78.

(31) Belov, V.; Wurm, C.; Boyarskiy, V.; Jakobs, S.; Hell, S. Rhodamines NN: A novel class of caged fluorescent dyes. *Angew. Chem., Int. Ed.* **2010**, *49*, 3520−3523.
(32) Banala, S.; Maurel, D.; Manley, S.; Johnsson, K. A caged, localizable rhodamine for superresolution microscopy. *ACS Chem. Biol.* **2012**, *7*, 289−293.
(33) Wysocki, L. M.; Grimm, J. B.; Tkachuk, A. N.; Brown, T. A.; Betzig, E.; Lavis, L. D. Facile and general synthesis of photoactivatable xanthene dyes. *Angew. Chem., Int. Ed.* **2011**, *50*, 11206−11209.
(34) Belov, V. N.; Mitronova, G. Y.; Bossi, M. L.; Boyarskiy, V. P.; Hebisch, E.; Geisler, C.; Kolmakov, K.; Wurm, C. A.; Willig, K. I.; Hell, S. W. Masked rhodamine dyes of five principal colors revealed by photolysis of a 2-diazo-1-indanone caging group: Synthesis, photophysics, and light microscopy applications. *Chem. - Eur. J.* **2014**, *20*, 13162−13173.
(35) Grimm, J. B.; English, B. P.; Choi, H.; Muthusamy, A. K.; Mehl, B. P.; Dong, P.; Brown, T. A.; Lippincott-Schwartz, J.; Liu, Z.; Lionnet, T.; Lavis, L. D. Bright photoactivatable fluorophores for single-molecule imaging. *Nat. Methods* **2016**, *13*, 985−988.
(36) Grimm, J. B.; Heckman, L. M.; Lavis, L. D. The chemistry of small-molecule fluorogenic probes. *Prog. Mol. Biol. Transl. Sci.* **2013**, *113*, 1−34.
(37) Arden-Jacob, J.; Frantzeskos, J.; Kemnitzer, N. U.; Zilles, A.; Drexhage, K. H. New fluorescent markers for the red region. *Spectrochim. Acta, Part A* **2001**, *57*, 2271−2283.
(38) Kolmakov, K.; Belov, V. N.; Wurm, C. A.; Harke, B.; Leutenegger, M.; Eggeling, C.; Hell, S. W. A versatile route to red-emitting carbopyronine dyes for optical microscopy and nanoscopy. *Eur. J. Org. Chem.* **2010**, *2010*, 3593−3610.
(39) Kolmakov, K.; Wurm, C.; Sednev, M. V.; Bossi, M. L.; Belov, V. N.; Hell, S. W. Masked red-emitting carbopyronine dyes with photosensitive 2-diazo-1-indanone caging group. *Photochem. Photobiol. Sci.* **2012**, *11*, 522−532.
(40) Grimm, J. B.; Sung, A. J.; Legant, W. R.; Hulamm, P.; Matlosz, S. M.; Betzig, E.; Lavis, L. D. Carbofluoresceins and carborhodamines as scaffolds for high-contrast fluorogenic probes. *ACS Chem. Biol.* **2013**, *8*, 1303−1310.
(41) Grimm, J. B.; Gruber, T. D.; Ortiz, G.; Brown, T. A.; Lavis, L. D. Virginia Orange: A versatile, red-shifted fluorescein scaffold for single- and dual-input fluorogenic probes. *Bioconjugate Chem.* **2016**, *27*, 474−480.
(42) Fu, M.; Xiao, Y.; Qian, X.; Zhao, D.; Xu, Y. A design concept of long-wavelength fluorescent analogs of rhodamine dyes: Replacement of oxygen with silicon atom. *Chem. Commun.* **2008**, 1780−1782.
(43) Egawa, T.; Koide, Y.; Hanaoka, K.; Komatsu, T.; Terai, T.; Nagano, T. Development of a fluorescein analogue, TokyoMagenta, as a novel scaffold for fluorescence probes in red region. *Chem. Commun.* **2011**, *47*, 4162−4164.
(44) Koide, Y.; Urano, Y.; Hanaoka, K.; Terai, T.; Nagano, T. Evolution of Group 14 rhodamines as platforms for near-infrared fluorescence probes utilizing photoinduced electron transfer. *ACS Chem. Biol.* **2011**, *6*, 600−608.
(45) Egawa, T.; Hanaoka, K.; Koide, Y.; Ujita, S.; Takahashi, N.; Ikegaya, Y.; Matsuki, N.; Terai, T.; Ueno, T.; Komatsu, T.; Nagano, T. Development of a far-red to near-infrared fluorescence probe for calcium ion and its application to multicolor neuronal imaging. *J. Am. Chem. Soc.* **2011**, *133*, 14157−14159.
(46) Lukinavičius, G.; Umezawa, K.; Olivier, N.; Honigmann, A.; Yang, G.; Plass, T.; Mueller, V.; Reymond, L.; Corrêa, I. R., Jr.; Luo, Z. G.; Schultz, C.; Lemke, E. A.; Heppenstall, P.; Eggeling, C.; Manley, S.; Johnsson, K. A near-infrared fluorophore for live-cell super-resolution microscopy of cellular proteins. *Nat. Chem.* **2013**, *5*, 132−139.
(47) Lukinavičius, G.; Reymond, L.; D'Este, E.; Masharina, A.; Gottfert, F.; Ta, H.; Guther, A.; Fournier, M.; Rizzo, S.; Waldmann, H.; Blaukopf, C.; Sommer, C.; Gerlich, D. W.; Arndt, H.-D.; Hell, S. W.; Johnsson, K. Fluorogenic probes for live-cell imaging of the cytoskeleton. *Nat. Methods* **2014**, *11*, 731−733.
(48) Erdmann, R. S.; Takakura, H.; Thompson, A. D.; Rivera-Molina, F.; Allgeyer, E. S.; Bewersdorf, J.; Toomre, D.; Schepartz, A. Super-resolution imaging of the Golgi in live cells with a bioorthogonal ceramide probe. *Angew. Chem., Int. Ed.* **2014**, *53*, 10242−10246.
(49) Hirabayashi, K.; Hanaoka, K.; Takayanagi, T.; Toki, Y.; Egawa, T.; Kamiya, M.; Komatsu, T.; Ueno, T.; Terai, T.; Yoshida, K.; Uchiyama, M.; Nagano, T.; Urano, Y. Analysis of chemical equilibrium of silicon-substituted fluorescein and its application to develop a scaffold for red fluorescent probes. *Anal. Chem.* **2015**, *87*, 9061−9069.
(50) Lukinavičius, G.; Blaukopf, C.; Pershagen, E.; Schena, A.; Reymond, L.; Derivery, E.; Gonzalez-Gaitan, M.; D'Este, E.; Hell, S. W.; Gerlich, D. W.; Johnsson, K. SiR-Hoechst is a far-red DNA stain for live-cell nanoscopy. *Nat. Commun.* **2015**, *6*, 8497.
(51) Kushida, Y.; Nagano, T.; Hanaoka, K. Silicon-substituted xanthene dyes and their applications in bioimaging. *Analyst* **2015**, *140*, 685−695.
(52) Huang, Y.-L.; Walker, A. S.; Miller, E. W. A photostable silicon rhodamine platform for optical voltage sensing. *J. Am. Chem. Soc.* **2015**, *137*, 10767−10776.
(53) Lukinavicius, G.; Reymond, L.; Umezawa, K.; Sallin, O.; D'Este, E.; Gottfert, F.; Ta, H.; Hell, S. W.; Urano, Y.; Johnsson, K. Fluorogenic probes for multicolor imaging in living cells. *J. Am. Chem. Soc.* **2016**, *138*, 9365−9368.
(54) Grimm, J. B.; Klein, T.; Kopek, B. G.; Hess, H. F.; Sauer, M.; Lavis, L. D.; Shtengel, G. Synthesis of a far-red photoactivatable Si-rhodamine for super resolution microscopy. *Angew. Chem., Int. Ed.* **2016**, *55*, 1723−1727.
(55) Kolmakov, K.; Hebisch, E.; Wolfram, T.; Nordwig, L. A.; Wurm, C. A.; Ta, H.; Westphal, V.; Belov, V. N.; Hell, S. W. Far-red emitting fluorescent dyes for optical nanoscopy: Fluorinated silicon-rhodamines (SiRF dyes) and phosphorylated oxazines. *Chem. - Eur. J.* **2015**, *21*, 13344−13356.
(56) Zhou, X.; Lai, R.; Beck, J. R.; Li, H.; Stains, C. I. Nebraska Red: A phosphinate-based near-infrared fluorophore scaffold for chemical biology applications. *Chem. Commun.* **2016**, *52*, 12290−12293.
(57) Chai, X.; Cui, X.; Wang, B.; Yang, F.; Cai, Y.; Wu, Q.; Wang, T. Near-Infrared phosphorus-substituted rhodamine with emission wavelength above 700 nm for bioimaging. *Chem. - Eur. J.* **2015**, *21*, 16754−16758.
(58) Liu, J.; Sun, Y. Q.; Zhang, H.; Shi, H.; Shi, Y.; Guo, W. Sulfone-Rhodamines: A new class of near-infrared fluorescent dyes for bioimaging. *ACS Appl. Mater. Interfaces* **2016**, *8*, 22953−22962.
(59) Roth, A.; Li, H.; Anorma, C.; Chan, J. A reaction-based fluorescent probe for imaging of formaldehyde in living cells. *J. Am. Chem. Soc.* **2015**, *137*, 10890−10893.
(60) Brewer, T. F.; Chang, C. J. An aza-cope reactivity-based fluorescent probe for imaging formaldehyde in living cells. *J. Am. Chem. Soc.* **2015**, *137*, 10886−10889.
(61) Krishnamoorthy, L.; Cotruvo, J. A., Jr.; Chan, J.; Kaluarachchi, H.; Muchenditsi, A.; Pendyala, V. S.; Jia, S.; Aron, A. T.; Ackerman, C. M.; Wal, M. N.; Guan, T.; Smaga, L. P.; Farhi, S. L.; New, E. J.; Lutsenko, S.; Chang, C. J. Copper regulates cyclic-AMP-dependent lipolysis. *Nat. Chem. Biol.* **2016**, *12*, 586−592.
(62) Ticau, S.; Friedman, L. J.; Ivica, N. A.; Gelles, J.; Bell, S. P. Single-molecule studies of origin licensing reveal mechanisms ensuring bidirectional helicase loading. *Cell* **2015**, *161*, 513−525.
(63) Li, L.; Liu, H.; Dong, P.; Li, D.; Legant, W. R.; Grimm, J. B.; Lavis, L. D.; Betzig, E.; Tjian, R.; Liu, Z. Real-time imaging of Huntingtin aggregates diverting target search and gene transcription. *eLife* **2016**, *5*, e17056.
(64) Morisaki, T.; Lyon, K.; DeLuca, K. F.; DeLuca, J. G.; English, B. P.; Zhang, Z. J.; Lavis, L. D.; Grimm, J. B.; Viswanathan, S.; Looger, L. L.; Lionnet, T.; Stasevich, T. J. Real-time quantification of single RNA translation dynamics in living cells. *Science* **2016**, *352*, 1425−1429.
(65) Wang, B.; Chai, X.; Zhu, W.; Wang, T.; Wu, Q. A general approach to spirolactonized Si-rhodamines. *Chem. Commun.* **2014**, *50*, 14374−14377.
(66) During the preparation of this manuscript, an alternative preparation of a similar Si-anthrone (Y = OTIPS) was reported (ref 17).

DOI: 10.1021/acscentsci.7b00247
ACS Cent. Sci. 2017, 3, 975−985

(67) Sun, W.-C.; Gee, K. R.; Klaubert, D. H.; Haugland, R. P. Synthesis of fluorinated fluoresceins. *J. Org. Chem.* **1997**, *62*, 6469−6475.
(68) Prober, J. M.; Trainor, G. L.; Dam, R. J.; Hobbs, F. W.; Robertson, C. W.; Zagursky, R. J.; Cocuzza, A. J.; Jensen, M. A.; Baumeister, K. A system for rapid DNA sequencing with fluorescent chain-terminating dideoxynucleotides. *Science* **1987**, *238*, 336−341.
(69) Hinckley, D. A.; Seybold, P. G.; Borris, D. P. Solvatochromism and thermochromism of rhodamine solutions. *Spectrochim. Acta, Part A* **1986**, *42*, 747−754.
(70) Hinckley, D. A.; Seybold, P. G. Thermodynamics of the rhodamine B lactone−zwitterion equilibrium. An undergraduate laboratory experiment. *J. Chem. Educ.* **1987**, *64*, 362−364.
(71) Yang, Y.; Escobedo, J. O.; Wong, A.; Schowalter, C. M.; Touchy, M. C.; Jiao, L.; Crowe, W. E.; Fronczek, F. R.; Strongin, R. M. A convenient preparation of xanthene dyes. *J. Org. Chem.* **2005**, *70*, 6907−6912.
(72) Yang, Y.; Lowry, M.; Xu, X.; Escobedo, J. O.; Sibrian-Vazquez, M.; Wong, L.; Schowalter, C. M.; Jensen, T. J.; Fronczek, F. R.; Warner, I. M.; Strongin, R. M. Seminaphthofluorones are a family of water-soluble, low molecular weight, NIR-emitting fluorophores. *Proc. Natl. Acad. Sci. U. S. A.* **2008**, *105*, 8829−8834.
(73) Chan, D. M. T.; Monaco, K. L.; Wang, R. P.; Winters, M. P. New N- and O-arylations with phenylboronic acids and cupric acetate. *Tetrahedron Lett.* **1998**, *39*, 2933−2936.
(74) Evans, D. A.; Katz, J. L.; West, T. R. Synthesis of diaryl ethers through the copper-promoted arylation of phenols with arylboronic acids. An expedient synthesis of thyroxine. *Tetrahedron Lett.* **1998**, *39*, 2937−2940.
(75) Qiao, J. X.; Lam, P. Y. S. Copper-promoted carbon-heteroatom bond cross-coupling with boronic acids and derivatives. *Synthesis* **2011**, *2011*, 829−856.
(76) Anzalone, A. V.; Chen, Z.; Cornish, V. W. Synthesis of photoactivatable azido-acyl caged oxazine fluorophores for live-cell imaging. *Chem. Commun.* **2016**, *52*, 9442−9445.
(77) Gee, K. R.; Sun, W. C.; Klaubert, D. H.; Haugland, R. P.; Upson, R. H.; Steinberg, T. H.; Poot, M. Novel derivatization of protein thiols with fluorinated fluoresceins. *Tetrahedron Lett.* **1996**, *37*, 7905−7908.
(78) Greenspan, P.; Fowler, S. Spectrofluorometric studies of the lipid probe, nile red. *J. Lipid Res.* **1985**, *26*, 781−789.

DOI: 10.1021/acscentsci.7b00247
ACS Cent. Sci. 2017, 3, 975−985